

---

# Elimination of the Influence of Total Renal Function on Renal Output Efficiency and Normalized Residual Activity

Cyril C. Nimmon, BSc<sup>1</sup>; Martin Šámal, PhD<sup>2</sup>; and Keith E. Britton, MD<sup>3</sup>

<sup>1</sup>Chiang Mai, Thailand; <sup>2</sup>Institute of Nuclear Medicine, 1st Faculty of Medicine, Charles University Prague, Prague, Czech Republic; and <sup>3</sup>Department of Nuclear Medicine, St. Bartholomew's Hospital, London, United Kingdom

One of the potential limitations in the usefulness of both renal output efficiency (ROE) and normalized residual activity (NORA) is their residual dependence on total renal function. The purpose of this study was to present and examine a new quantitative method whereby the effects of this dependence may be removed. **Methods:** The analytic method involves the determination of a retention function using an unconstrained matrix algorithm deconvolution technique followed by reconvolution with a chosen standard input function to yield a new secondary renal activity time (A/T) curve from which normalized values of ROE and NORA, denoted as N\_ROE and N\_NORA, respectively, can then be obtained using conventional definitions. The method has been applied in a series of 50 patient studies, which had been acquired using <sup>99m</sup>Tc-mercaptoacetyltryglycine (<sup>99m</sup>Tc-MAG3) and a standard F+18 furosemide protocol, with values of the ratio of plasma clearance to plasma volume (C/V) in the range 0.013–0.242 min<sup>-1</sup>. **Results:** Pre- and postnormalization values of NORA, calculated at 30 min after injection, showed a significant difference in mean values (paired *t* test; *P* < 0.001), with a maximum observed difference, ΔNORA(30), of -4.82 (-482%) and with a SD on the paired differences, ΔNORA(30), of 0.56 (56%) or 0.63 (63%) if background subtraction on the input function (BSIF) had been performed. In contrast, corresponding values of ROE showed a nonsignificant difference in means (*P* > 0.05) and a SD on the paired differences, ΔROE(30), of 3.7% or 3.2% with and without BSIF, respectively. The normalized parameters N\_ROE and N\_NORA were found to be strongly linearly correlated (*r* = -0.99; *P* < 0.001), in agreement with theoretical predictions. **Conclusion:** These results suggest that renal function affects NORA significantly more than ROE. The effects can be corrected by our normalization technique, resulting in equivalent values of normalized ROE and normalized NORA.

**Key Words:** dynamic renal study; output efficiency; normalized residual activity; deconvolution

**J Nucl Med 2004; 45:587–593**

**T**he quantitative parameter renal output efficiency (ROE) was developed over a decade ago with the aim of improving the diagnostic accuracy of the assessment of the furosemide response in diuresis renography (1–3). Clinical studies following protocols in which ROE is calculated at 30 min after the start of an F+18, F+15, or F+20 furosemide study have provided evidence validating the usefulness of this parameter both in adults (2,4) and in children (5). The general concept of ROE as a measure of renal emptying has potentially an even wider use. ROE may be calculated at various times into the renal study and may also be applied to nonfurosemide studies. Reported applications have included the assessment of the utility of parenchymal activity time (A/T) curves in the prediction of the furosemide response (6).

Possible limitations in the accuracy of ROE have been suggested due, for example, to its residual dependence on total renal function and on the use of a curve derived from a region of interest (ROI) placed posteriorly over a left ventricular region as representative of the plasma disappearance curve (7–9). ROE expresses the total renal output up to a time *t* as a percentage of the total input occurring up to that time. Any apparent residual dependence of ROE on the total renal function must therefore arise from a difference in shape of the input function rather than from a difference in the total input. Variation in the shape of the input function represents variation in the time course of renal input, which in turn leads to a difference in levels of occupancy of the individual transit time pathways through the system at the time of measurement of ROE. This difference in occupancy of the transit time pathways at the time of measurement will be apparent in the value of the background-subtracted renal A/T curve *R'(t)*. The dependence of *R'(t)* on the shape of the background-subtracted input A/T curve *P'(t)* is in fact embodied in the convolution equation:

$$R'(t) = P'(t) * H(t), \quad \text{Eq. 1}$$

where \* denotes the convolution operator. *H(t)* is the renal impulse retention function (RF) and is a characteristic of the particular kidney subject to the conditions of linearity and

---

Received Sep. 30, 2003; revision accepted Dec. 2, 2003.  
For correspondence or reprints contact: Cyril C. Nimmon, P.O. Box 12, Bor Sang, Sankampaeng, Chiang Mai 50131, Thailand.  
E-mail: hermesnc@cscoms.com

stationarity. (The RF may be defined as the A/T curve that would be observed after administration of activity in the form of a unit impulse into the renal artery and without any subsequent recirculation of tracer.)

Another parameter of renal emptying is the normalized residual activity, (NORA) (10,11). NORA expresses the renal activity  $R'(t)$  at time  $t$  in terms of the renal activity between 1 to 2 min. Since the value of  $R'(t)$  is used in the calculation of both ROE and NORA, it is reasonable to expect that both of these parameters will exhibit a residual dependence on total renal function (12).

The aim of this study was to propose, and examine the application of, a new method for normalization of both the parameters ROE and NORA, which renders values independent of variations in the shape of the input function due to different levels of renal function.

## MATERIALS AND METHODS

### Patient Studies

A series of 50 dynamic renal studies, using  $^{99m}\text{Tc}$ -mercaptoacetyltriglycine ( $^{99m}\text{Tc}$ -MAG3), were selected from the clinical database of the Department of Nuclear Medicine, St. Bartholomew's Hospital, London, U.K. The majority of the adult patients chosen had been referred as part of a routine investigation of the upper urinary tract with a high suspicion of possible outflow tract disorder. The studies were performed between 1992 and 1996 and were recorded following a standard F+ 18 furosemide protocol in which 40 mg of furosemide were administered 18 min after a bolus intravenous injection of 100 MBq  $^{99m}\text{Tc}$ -MAG3. The procedures used had been approved by the local ethical committee. All studies were performed with the patient in the sitting position reclining with his or her back to the face of a  $\gamma$ -camera fitted with a general-purpose collimator, which was inclined backward at approximately  $10^\circ$ – $20^\circ$  to the vertical. The camera was positioned so that the region of the left ventricle as well as both kidneys were within the field of view. Each study consisted of 180 images,  $64 \times 64$  pixels, recorded at 10-s intervals. Subsequent data analysis was performed using a Hermes nuclear medicine computer system (Nuclear Diagnostics AB).

### Calculation of ROE and NORA

From the 50 patient studies, a total of 96 individual kidneys were analyzed, 4 kidneys being excluded because of either absent or extremely low renal uptake function. For each of the 96 kidneys, the whole kidney A/T curve was obtained corresponding to a manually drawn irregular ROI. This renal A/T curve was first corrected for extrarenal background activity using a lateral C-shaped perirenal ROI and then further corrected for intrarenal vascular background activity using the Patlak–Rutland plot (13). An input A/T curve,  $P(t)$ , was obtained from a ROI positioned over the left ventricle. Extravascular background was subtracted from  $P(t)$  using a method derived from the technique suggested by Fleming (14). Following the Fleming technique, after correction for ROI size, a fraction  $k$  of the A/T curve obtained from a ROI positioned between the upper poles of the kidneys was subtracted from  $P(t)$ . In the current study using MAG3, it was found that by choosing a value of 0.49 for  $k$ , the results obtained for ROE correlated closely ( $P < 0.001$ ) with those obtained using the Bell–Peters method (15). The background-subtracted input curve,

$P'(t)$ , was taken as being representative of the plasma clearance curve. An iterative least-squares technique was then used to fit the integral of  $P'(t)$  to a part of the upstroke of  $R'(t)$  (2). The difference between the fitted curve,  $I(t)$ , and  $R'(t)$  yielded a curve representing the total output of the kidney up to time  $t$ , which, when expressed as a percentage of the total input up to that time, gave the output efficiency  $\text{ROE}(t)$ :

$$\text{ROE}(t) = [I(t) - R'(t)] \cdot 100/[I(t)]. \quad \text{Eq. 2}$$

Values of ROE at a specific time  $t_2 = 30$  min—namely,  $\text{ROE}(30)$ —were obtained by averaging  $\text{ROE}(t)$  over a 1-min period. For the purpose of evaluation of the effect of background subtraction on the input function (BSIF), values for  $\text{ROE}(30)$  were also calculated by substitution of the curve  $P(t)$  in place of  $P'(t)$ .  $\text{NORA}(t_2)$  was calculated as the ratio between the values of  $R'(t_2)$ , averaged over a 1-min period, and  $R'(2)$ , being the average value of  $R'(t)$  between 1 and 2 min:

$$\text{NORA}(t_2) = [R'(t_2)]/[R'(2)]. \quad \text{Eq. 3}$$

Values of  $\text{NORA}(t_2)$  were calculated for  $t_2 = 30$  min—namely,  $\text{NORA}(30)$ . For both ROE and NORA, the time corresponding to  $t = 0$ , was taken at the initial maximum in the input curve,  $P'(t)$ .

### Theoretical Relationship Between ROE and NORA

For ease of comparison with  $\text{ROE}(t_2)$ , the ratio  $\text{NORA}(t_2)$  can be expressed as a percentage and written as  $\text{NORA}(2, t_2)$ :

$$\text{NORA}(2, t_2) = [R'(t_2)] \cdot 100/[R'(2)]. \quad \text{Eq. 4}$$

Since  $R'(t)$  is fitted to the integral of the input function in the neighborhood of 2 min,

$$R'(2) \approx I(2),$$

and

$$\text{NORA}(2, t_2) = [R'(t_2)] \cdot 100/[I(2)]. \quad \text{Eq. 5}$$

$\text{NORA}(2, t_2)$ , as defined by Equation 5, can be thought of as the residual activity at time  $t_2$  expressed as a percentage of the total input occurring up to a time of 2 min. Similarly, the residual activity at time  $t_2$  expressed as a percentage of the total input occurring up to time  $t_1$  minutes can be described by the more general parameter  $\text{NORA}(t_1, t_2)$ :

$$\text{NORA}(t_1, t_2) = [R'(t_2)] \cdot 100/[I(t_1)]. \quad \text{Eq. 6}$$

In particular, one may choose  $t_1 = t_2$ . Then by rearranging the variables in Equation 6 and substituting for  $R'(t_2)$  in Equation 5:

$$\text{NORA}(2, t_2) = [I(t_2)] \cdot \text{NORA}(t_2, t_2)/[I(2)]. \quad \text{Eq. 7}$$

From Equations 2 and 6, setting the value of  $t = t_1 = t_2$ ,

$$\text{NORA}(t_2, t_2) = 100 - \text{ROE}(t_2). \quad \text{Eq. 8}$$

Hence,

$$\text{NORA}(2, t_2) = [I(t_2)] \cdot [100 - \text{ROE}(t_2)]/[I(2)], \quad \text{Eq. 9}$$

and

$$\text{ROE}(t_2) = 100 - [I(2)] \cdot [\text{NORA}(2, t_2)]/[I(t_2)]. \quad \text{Eq. 10}$$

Equations 9 and 10 describe a linear relationship between the values of NORA and ROE for an individual renal study. In

general, the ratio  $I(t_2)/I(2)$  will depend on the shape of the input curve and thus will exhibit a dependence on plasma clearance.

### Deconvolution–Convolution Method for Normalization of ROE and NORA

Normalization of both ROE and NORA to a standard input curve represents a technique for removing the dependence on the plasma clearance as reflected in both  $R'(t_2)$  and the ratio  $I(t_2)/I(2)$ . After such normalization, Equations 9 and 10 should provide simple formulas enabling either ROE or NORA to be calculated from each other.

*Algorithm.* The first step of the method is to obtain the RF,  $H(t)$ , by deconvolution of the background-subtracted renal curve  $R'(t)$  using  $P'(t)$  as the input function. Second, convolution of  $H(t)$  with a chosen standard input curve,  $SP'(t)$ , is performed to yield a new renal A/T curve  $R_c'(t)$ :

$$R_c'(t) = SP'(t) * H(t). \quad \text{Eq. 11}$$

The integral of  $SP'(t)$  is fitted to the upstroke of  $R_c'(t)$  as described previously and normalized values of ROE( $t_2$ ) and NORA( $t_2$ ), denoted as  $N_{ROE}(t_2)$  and  $N_{NORA}(t_2)$ , respectively, are then calculated according to Equations 2 and 3 using  $R_c'(t)$  along with the new values for  $I(2)$  and  $I(t_2)$ .

Usually both linearity and stationarity for the system are important requirements for the application of deconvolution and are taken to exclude the use of deconvolution within a time period of the renal study in which nonstationary events are known to occur—for example, due to irregular emptying of the renal pelvis or the administration of a diuretic such as furosemide. However, it is proposed that the strict requirement of stationarity may be relaxed provided that quantitative parameters such as renal transit times are not calculated from the RF. For example, in a furosemide study, if deconvolution is applied in the region of nonstationarity, the resulting RF can be termed a “virtual RF” and is likely to contain nonphysiologic negative values.

These negative values represent an encoding into the RF of the nonstationarity and are required to ensure an accurate reconstruction of the observed renal curve  $R'(t)$  by convolution with the input function.

When a different standard input function  $SP'(t)$  is used, the encoded nonstationarity is decoded into the resultant new renal curve  $R_c'(t)$ , commencing at the same time point as in the original curve. To allow for the use of either a real or a virtual RF in Equation 11, it is important that the method of deconvolution used to calculate  $H(t)$  is unconstrained. Although methods of deconvolution incorporating constraints, such as those of nonnegativity and monotonicity, for example, are advantageous for the calculation of transit times (16–22), they may lead to significant reconvolution errors in a region of nonstationarity.

*Technical Details.* Before deconvolution using an unconstrained matrix method of deconvolution, the renal A/T curves  $R'(t)$  were first subjected to five 1–2–1 weighted smooths. To ensure stability of the deconvolution, any leading edge in the input curve was set to zero so that the first nonzero point in the input curve was the highest point (17,18). After deconvolution, the RF curves were subjected to one 1–2–1 weighted smooth. A first derivative gradient method, supplemented by a manual visual method as necessary, was used to detect the initial plateau and any residual contribution above the plateau, arising from incomplete prior removal of extravascular or vascular renal background from  $R'(t)$ , was removed before convolution of  $H(t)$  with the standard input curve.

*Standard Input Curve.* The standard input curve,  $SP'(t)$ , was chosen from the dataset on the basis of a value for the ratio of MAG3 clearance ( $C$ , mL/min) to plasma volume ( $V$ , mL) of  $>0.15 \text{ min}^{-1}$  and a low level of noise on the original data. The chosen curve was then subjected to a triexponential fit both before and after background subtraction to obtain the parameters shown in Table 1:

$$SP'(t) = a_0 \exp[-b_0 t] + a_1 \exp[-b_1 t] + a_2 \exp[-b_2 t]. \quad \text{Eq. 12}$$

### Estimation of Plasma Clearance

Values of the ratio  $C/V$  were obtained from a 2-exponential model fit to the background-subtracted heart curves  $P'(t)$ . The exponential components were fitted using a method analogous to a graphical stripping technique (23), which yielded values for intercepts  $a_1$ ,  $a_2$  and exponents  $b_1$ ,  $b_2$ , respectively:

$$P'(t) = a_1 \exp[-b_1 t] + a_2 \exp[-b_2 t]. \quad \text{Eq. 13}$$

The area under the clearance curve,  $A_r$  is given by:

$$A_r = [a_1/b_1] + [a_2/b_2], \quad \text{Eq. 14}$$

and using the standard formula appropriate to the single injection technique (24):

$$C/V = [(a_1 + a_2)]/A_r. \quad \text{Eq. 15}$$

The ratio  $C/V$  has units of  $\text{minutes}^{-1}$  and represents the fraction of the plasma volume cleared per minute. Such measures of clearance in terms of body spaces have an advantage in that they do not require further corrections based on individual patient dimensions (25).

## RESULTS

### Estimation of Plasma Clearance

The values for the ratio  $C/V$ , which were obtained from the 50 studies, had a range of 0.013–0.242  $\text{min}^{-1}$  and a mean  $\pm$  SD of  $0.12 \pm 0.044 \text{ min}^{-1}$ .

### Data Analysis Before Normalization

As shown in Figure 1, values for ROE(30) after BSIF were linearly correlated with the corresponding values before BSIF ( $r = 0.994$ ;  $P < 0.001$ ), and the difference between the means was significant (paired  $t$  test;  $P <$

**TABLE 1**  
Parameters Derived from Triexponential Fit to Chosen Standard Input Function With and Without Prior Subtraction of Extravascular Background

Background subtracted	$a_0$	$a_1$	$a_2$	$b_0$ ( $\text{min}^{-1}$ )	$b_1$ ( $\text{min}^{-1}$ )	$b_2$ ( $\text{min}^{-1}$ )
No [SP(t)]	0.685	0.179	0.136	4.79	0.318	0.036
Yes [SP'(t)]	0.746	0.163	0.091	4.62	0.495	0.058

Standard input function before and after subtraction of extravascular background is denoted by  $SP(t)$  and  $SP'(t)$ , respectively.  $SP(t)$  [or  $SP'(t)$ ] =  $a_0 \exp[-b_0 t] + a_1 \exp[-b_1 t] + a_2 \exp[-b_2 t]$ , where input functions have been adjusted to initial maximum of unity at time  $t = 0$ .

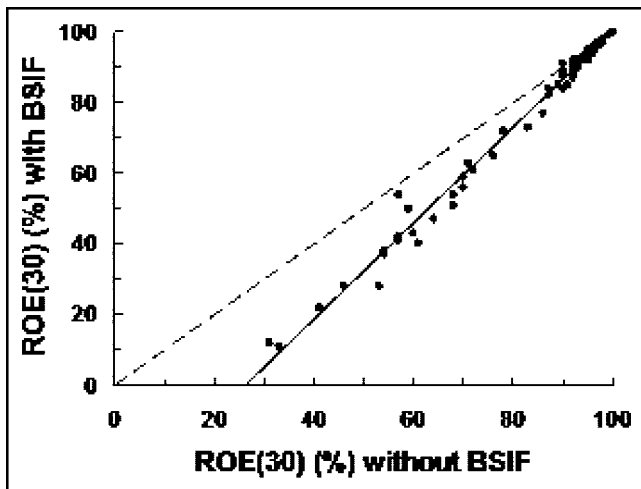


**FIGURE 1.** Correlation of ROE(30) obtained after subtraction of background from input function (with BSIF) ( $y$ -axis) with corresponding values obtained without any subtraction of background from input function (without BSIF) ( $x$ -axis).  $y = 1.357x - 34.77$ ; coefficient of linear correlation,  $r = 0.994$ . Dashed line represents line of identity.

0.001). The effect of BSIF was to reduce the value of ROE(30). Since NORA(30) was calculated using only data from  $R'(t)$ , values of NORA(30) were unaffected by BSIF.

Examination of both the nonconstant nature of the ratio  $I(30)/I(2)$  and the deviation from a linear relationship between ROE and NORA have been used to illustrate the need for normalization in the dataset used in this study. Values for the ratio  $I(30)/I(2)$  were calculated from the BSIF data. As anticipated theoretically, the ratio was found to exhibit significant variation with the estimated plasma clearance as shown in Figure 2. The ratio  $I(30)/I(2)$  showed a positively skewed distribution (range, 3.3–12.4; mean  $\mu$ , 5.02; SD, 1.67) with the highest value ( $\approx 2.4 \times \mu$ ) corresponding to the lowest value of clearance ( $C/V \approx 0.013 \text{ min}^{-1}$ ). Values significantly higher than  $\mu$  lead to the possibility of over-

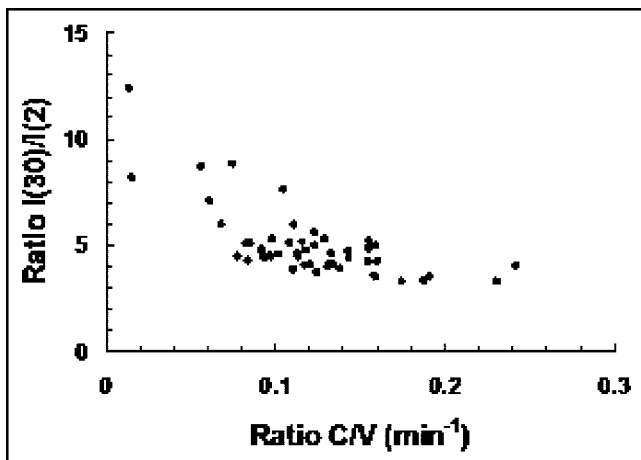


**FIGURE 2.** Variation of ratio  $I(30)/I(2)$  ( $y$ -axis) with ratio  $C/V$  ( $\text{min}^{-1}$ ) ( $x$ -axis).

estimation of NORA if predicted from ROE or, conversely, an underestimation of ROE if predicted from NORA using Equations 9 and 10, respectively. Some of this variation in the ratio  $I(30)/I(2)$  was reflected in the comparison of the values for ROE(30) and NORA(30) (Fig. 3), which were obtained with BSIF but before normalization using the deconvolution–convolution technique. Excluding 2 apparent outlying data points with coordinates ( $x, y$ ) of (388, 57) and (657, 47), respectively, the remaining data (94 values) showed a good linear correlation between ROE and NORA (coefficient of linear correlation,  $r = -0.97$ ;  $P < 0.001$ ), although with increasing dispersion for  $\text{ROE} < 60\%$ . However, the 2 outliers were found to be legitimate observations associated with high values of the ratio  $I(30)/I(2)$  of 8.9 and 12.4, respectively. All 96 data points have been included in subsequent analysis. The level of scatter of the data about the linear regression line shown in Figure 3 was given by SD residuals  $\sigma_y = 10.5\%$ ; SD residuals  $\sigma_x = 52.3\%$ , where  $\sigma_y = [\text{SD}_y] \cdot [\sqrt{1 - r^2}]$  and  $\sigma_x = [\text{SD}_x] \cdot \sqrt{1 - r^2}$ , respectively.

### Data Analysis After Normalization

*Analysis Using Input Function with Background Subtraction,  $SP'(t)$ :*

- After normalization, a comparison of  $N\_ROE(30)$  and  $N\_NORA(30)$  (Fig. 4) exhibited an excellent linear correlation ( $r = -0.998$ ;  $P < 0.001$ ) with very low residual scatter ( $\sigma_y = 1.3\%$ ;  $\sigma_x = 4.6\%$ ) as compared with the scatter observed before normalization ( $\sigma_y = 10.5\%$ ;  $\sigma_x = 52.3\%$ ), confirming the theoretical prediction of linearity expressed by Equation 10 and providing quantitative evidence of the success of the normalization procedure.

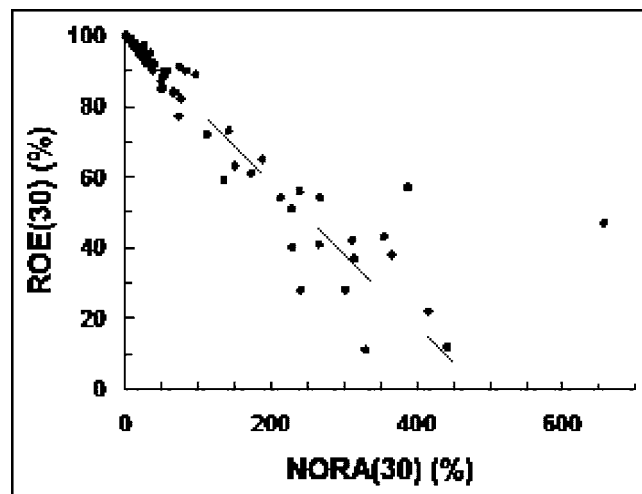


**FIGURE 3.** Comparison between ROE(30) ( $y$ -axis) and normalized residual activity NORA(30) expressed as a percentage ( $x$ -axis). Data are before normalization using deconvolution–convolution technique but after subtraction of background from input function. Solid line is regression line obtained excluding 2 outliers.  $y = -0.204x + 99.21$ ;  $r = -0.973$ .

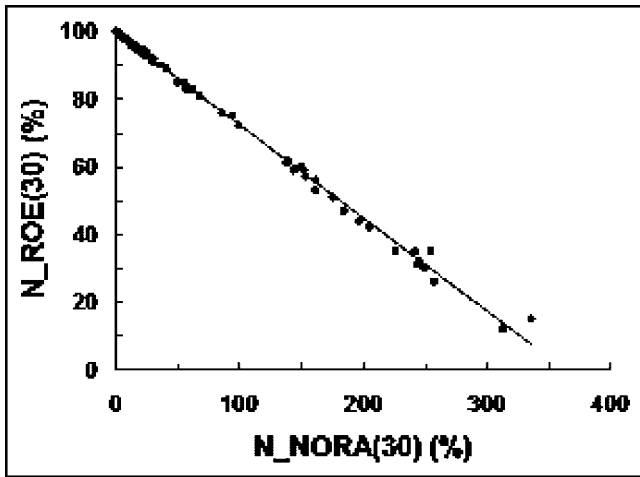


**FIGURE 4.** Comparison between normalized values N\_ROE(30) (y-axis) and N\_NORA(30) (x-axis), both calculated from data obtained after subtraction of background from input function.  $y = -0.2753x + 99.913$ ;  $r = -0.998$ .

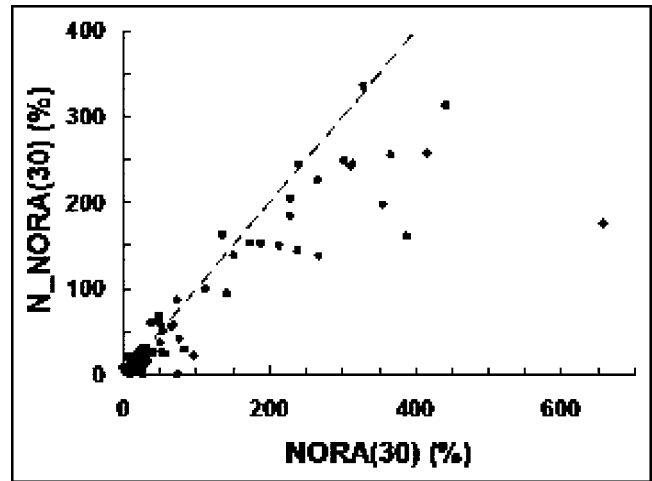


**FIGURE 6.** Comparison between normalized values N\_NORA(30) (y-axis) and prenormalization values of NORA(30) (x-axis), both calculated from data obtained after subtraction of background from input function. Dashed line represents line of identity.

- The effect of normalization on the individual parameters ROE and NORA was tested by the following 2 comparisons:
- A comparison of N\_ROE(30) with the prenormalization values of ROE(30) (Fig. 5) showed a good linear correlation close to the line of identity ( $r = 0.990$ ;  $P < 0.001$ ), with no significant difference between the means (paired  $t$  test;  $P > 0.1$ ). The mean difference  $\Delta\text{ROE}(30) = \text{N\_ROE}(30) - \text{ROE}(30)$  was 0.46% (SD = 3.2%), with a range between  $-7\%$  and  $+10\%$ .
- A comparison of N\_NORA(30) with NORA(30) is shown in Figure 6. Although the data in this graph exhibited a linear relationship for  $\text{NORA}(30) < 300\%$ , the inclusion of all data points led to an overall nonlinear pattern with a significant difference between the

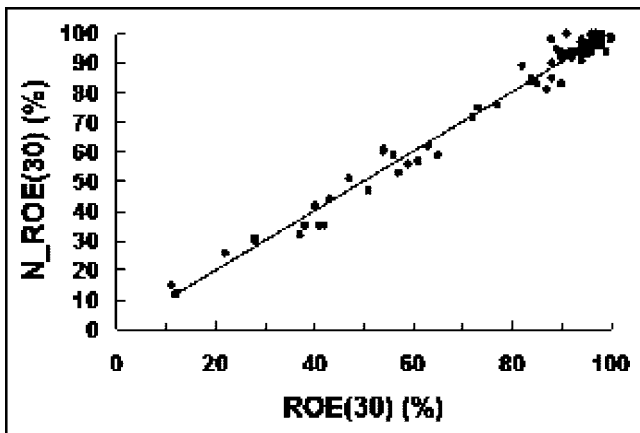


**FIGURE 5.** Comparison between normalized values N\_ROE(30) (y-axis) and prenormalization values of ROE(30) (x-axis), both calculated from data obtained after subtraction of background from input function.  $y = 1.0062x - 0.0486$ ;  $r = 0.99$ .

means (paired  $t$  test;  $P < 0.001$ ). The mean difference  $\Delta\text{NORA}(30) = \text{N\_NORA}(30) - \text{NORA}(30)$  was  $-26.5\%$  (SD = 62.5%), with a range between  $-482\%$  and  $+26\%$ .

*Analysis Using Input Function Without Background Subtraction, SP(t).* The results from normalization using the input function SP(t) exhibited features similar to those of the 3 paired items shown in Figures 4–6 but with slightly different numeric values for the regression coefficients and SDs as summarized:

- Comparison of N\_ROE(30) (y) and N\_NORA(30) (x) showed an excellent linear correlation, ( $y = -0.192x + 100.0$ ;  $r = -0.999$ ;  $P < 0.001$ ) and low residual scatter ( $\sigma_y = 0.53\%$ ;  $\sigma_x = 2.75\%$ ).
- Comparison of N\_ROE(30) (y) and ROE(30) (x) showed a good linear correlation, ( $y = 1.114x - 10.03$ ;  $r = 0.985$ ;  $P < 0.001$ ), a nonsignificant difference between the means (paired  $t$  test;  $P > 0.5$ ), and a low mean value of  $-0.14\%$  for  $\Delta\text{ROE}(30)$  with a corresponding SD of 3.7%.
- Comparison of N\_NORA(30) (y) and NORA(30) (x) showed a nonlinear pattern with significant difference between the means (paired  $t$  test;  $P < 0.001$ ) and a mean value of  $-20.4\%$  for  $\Delta\text{NORA}(30)$ , with a corresponding SD of 55.6%.
- These latter results obtained without using background subtraction on the input function are relevant to the procedures that have been used in the previously reported clinical applications of ROE(30) (2,4,5).

## DISCUSSION

In addition to presenting a method for the removal of the influence of variations in total renal function on the renal

output parameters ROE and NORA, this article has also examined the effects on these parameters of subtraction of extravascular background from the input function (BSIF).

The results show that, before normalization, BSIF has a significant effect on the values of ROE(30) but no effect on the values for NORA(30). This is because ROE depends on the measured or estimated plasma clearance A/T curve, whereas NORA depends on the actual but unknown plasma clearance curve. If the parameters are normalized, then BSIF affects both ROE and NORA since the measured plasma clearance A/T curve is used as the input function in the deconvolution procedure. From the results shown in Figure 1, BSIF clearly leads to a decrease in the values of ROE. The apparent disagreement with an article by Piepsz and Ham (8), which implied that the use of a plasma clearance curve instead of an A/T curve obtained from a heart ROI and without background subtraction should lead to an increase in ROE, is due to an inadvertent error in the text of that publication (Prof. Amy Piepsz, personal communication, written October 2002).

The decision as to whether to apply BSIF is an important one with potentially significant implications for many quantitative procedures such as measurements of plasma clearance, renal transit times, and renal output. The main theoretical advantage of performing this background subtraction is that, together with accurate background subtraction on the renal A/T curve, it leads to a closer approximation to the linear system model that lies at the basis of quantitative renal analysis. This advantage will have to be weighed against some apparent disadvantages such as the possible need to redefine normal or discriminant values for parameters that are already in use in clinically validated protocols. It is suggested that for MAG3, the regression parameters given in Figure 1 could be used to determine new discriminant levels for normal and equivocal values for ROE(30) from existing levels published for non-BSIF data (2,4,5). For example, discriminant levels identifying the lower limits of the normal and equivocal ranges for ROE(30) of 79% and 70%, respectively, for non-BSIF data would transform into corresponding values of 72% and 60%, respectively, for BSIF data.

The method of normalization presented in this article enables values to be obtained for both N\_ROE and N\_NORA, which are independent of total renal function. Either with or without BSIF, the effect of normalization on ROE has been found to be a nonsignificant difference in means as shown by a paired *t* test. The effect of the variation in plasma clearance on ROE is perhaps best described by the mean and SD of the difference,  $\Delta\text{ROE}(30) = \text{N\_ROE}(30) - \text{ROE}(30)$ , before and after normalization as described. Although the mean value of  $\Delta\text{ROE}(30)$  obtained from BSIF data is small ( $-0.85\%$ ), the possibility of an individual result having a significant difference is not excluded, as evidenced by a maximum observed value for  $|\Delta\text{ROE}(30)|$  of 10%. Simulations performed by Kuyvenhoven et al. (9), using plasma disappearance curves as the

input functions, have predicted a maximum SD on ROE(20) and ROE(40) of 6.2% and 8.4%, respectively, arising from variation in plasma clearance of MAG3 in the range 33–405 mL/min. The present study using patient data only, BSIF, and values of the ratio C/V in the range 0.013–0.242 min<sup>-1</sup> has shown a SD on ROE(30) of 3.2%, which is within the range predicted by the simulation studies and is correctable by normalization to a standard input function.

The mean value of  $-0.14\%$  obtained for  $\Delta\text{ROE}(30)$  from non-BSIF data implies that the same levels used for discrimination between normal and equivocal values of ROE(30) in the clinical furosemide study (2,4,5) can also be used after normalization.

Whether the process of normalization for ROE will prove to be a worthwhile procedure in clinical practice can probably be decided only by studying a larger set of patient studies together with an assessment of clinical outcome.

In contrast to ROE, the normalization procedure had a significant effect on NORA, as shown in the comparisons of N\_NORA(30) and NORA(30) (paired *t* test;  $P < 0.001$ ). Although the mean values of  $\Delta\text{NORA}(30)$ , ( $\Delta\text{NORA}(30) = \text{N\_NORA}(30) - \text{NORA}(30)$ ), were small ( $-20.2\%$  to  $-26.8\%$ ), the distribution of  $\Delta\text{NORA}(30)$  was negatively skewed with values up to  $-482\%$ . The largest values of  $|\Delta\text{NORA}(30)|$  were significantly greater than the corresponding values of  $|\Delta\text{ROE}(30)|$  and occurred at low values of total renal function. This would imply that ROE may be preferred in this situation if normalization were not undertaken for NORA.

In the case showing a value of  $\Delta\text{NORA}(30) = -482\%$ , both the initial value of NORA(30) of 657% and the normalized value N\_NORA(30) of 175% were within the abnormal range for NORA(30), and, in this instance, normalization would not have changed the clinical interpretation. However, it may be predicted that with a larger set of data results are likely to occur in which the value of NORA(30) would be in the abnormal range while the corresponding value of N\_NORA(30) would be in the normal range. By substitution of the observed values 47% and 657% for ROE(30) and NORA(30), respectively, in Equation 9, the value obtained for the ratio I(30)/I(2) is 12.40, which is a constant for this particular plasma clearance curve. Retaining this same value for the ratio I(30)/I(2), different pairs of values for ROE(30) and NORA(30) may then be simulated using Equation 9. As an example, one may consider the pair with values 80% and 248% for ROE(30) and NORA(30), respectively. After normalization, making use of the maximum range for ROE(30) found in this study, it may be predicted that the value for N\_ROE(30) should lie within the range 73%–90%. Using the value of 3.63 for the ratio I(30)/I(2) specific to the standard input curve, then the values for N\_NORA(30) corresponding to the possible limits of N\_ROE(30) may be calculated. Thus, it may be predicted that the resultant value for N\_NORA(30) would lie between 36% and 98%, which is clearly within the normal range, whereas the original value of NORA(30) was in the abnormal range.

Therefore, the procedure of normalization introduced in this article appears to be particularly advantageous for NORA since all of the wide variation due to difference in the shape of the input function is correctable.

For the technique of normalization to become applicable in different centers it will be necessary to agree on the actual input functions to be used—namely,  $SP'(t)$  and  $SP(t)$  for BSIF and non-BSIF data, respectively. Although there seems to be some degree of arbitrariness in the choice of the standard input function, the chosen curves should be within the bounds of possibility for the given study. Thus, it has been found necessary to use the curve  $SP(t)$  without subtraction of extravascular background for the non-BSIF data, rather than the background-subtracted curve  $SP'(t)$ , to avoid the occurrence of unphysical values for ROE(30) exceeding 100%.

When normalized, as described in this article, the 2 parameters  $N_{ROE}$  and  $N_{NORA}$  are seen to be closely related as predicted theoretically. They are as 2 sides of the same coin: One is concerned with the activity that has left the kidney and the other is concerned with the activity that remains.

## CONCLUSION

The results of this study demonstrate that the deconvolution–convolution normalization procedure introduced in this article, together with an appropriate choice of acquisition parameters and suitable renal background subtraction techniques, provides the means whereby equivalent values of normalized ROE and normalized NORA may be obtained. This study indicates that the level of plasma clearance affects ROE only to a minor degree, and from the available data it is not clear whether normalization of ROE will be found to be useful from the clinical point of view. On the other hand, the level of plasma clearance has a more marked affect on NORA, especially in cases of impaired renal function, and here normalization of NORA is more likely to prove advantageous. Further studies on a larger set of data should provide clarification of the usefulness of this technique.

## REFERENCES

1. Britton KE, Brown NJG, Nimmon CC. Clinical renography: 25 years on. *Eur J Nucl Med.* 1996;23:1541–1546.
2. Chaiwatanarat T, Padhy AK, Bomanji JB, Nimmon CC, Sonmezoglu K, Britton KE. Validation of renal output efficiency as an objective quantitative parameter

in the evaluation of upper urinary tract obstruction. *J Nucl Med.* 1993;34:845–848.

3. O'Reilly P, Aurell M, Britton K, Kletter K, Rosenthal L, Testa T. Consensus on diuresis renography for investigating the dilated upper urinary tract. *J Nucl Med.* 1996;37:1872–1876.
4. Jain S, Cosgriff PS, Turner DTL, Aslam M, Morrish O. Calculating the renal output efficiency as a method for clarifying equivocal renograms in adults with suspected upper urinary tract obstruction. *Br J Urol Int.* 2003;92:485–487.
5. Saunders CAB, Choong KKL, Larcos G, Farlow D, Gruenewald S. Assessment of paediatric hydronephrosis using output efficiency. *J Nucl Med.* 1997;38:1483–1486.
6. Šámal M, Bergmann H, Nimmon CC, Mostbeck A, Staudenherz A, Dudczak R. Utility of the whole-kidney and parenchymal time-activity curves for a prediction of diuretic response [abstract]. *Eur J Nucl Med.* 2002;29:S12.
7. Fleming JS, Kemp PM. A comparison of deconvolution and the Patlak-Rutland plot in renography analysis. *J Nucl Med.* 1999;40:1503–1507.
8. Piepsz A, Ham H. Factors influencing the accuracy of renal output efficiency. *Nucl Med Commun.* 2000;21:1009–1013.
9. Kuyvenhoven JD, Ham HR, Piepsz A. Influence of renal function on renal output efficiency. *J Nucl Med.* 2002;43:851–855.
10. Piepsz A, Tondeur M, Ham H. NORA: a simple and reliable parameter for estimating renal output with or without furosemide challenge. *Nucl Med Commun.* 2000;21:317–323.
11. Piepsz A, Kuyvenhoven JD, Tondeur M, Ham H. Normalized residual activity: usual values and robustness of the method. *J Nucl Med.* 2002;43:33–38.
12. Nimmon CC, Britton KE. Influence of renal function on renal output efficiency [letter]. *J Nucl Med.* 2003;44:658–659.
13. Rutland MD. A comprehensive analysis of renal DTPA studies. 1. Theory and normal values. *Nucl Med Commun.* 1985;6:11–20.
14. Fleming JS. Measurement of hippuran plasma clearance using a gamma camera. *Phys Med Biol.* 1977;22:526–530.
15. Bell SD, Peters AM. Extravascular chest wall technetium-99m diethylene triamine penta-acetic acid: implications for the measurement of renal function during renography. *Eur J Nucl Med.* 1991;18:87–90.
16. Lawson RS. Application of mathematical methods in dynamic nuclear medicine studies. *Phys Med Biol.* 1999;44:R57–R98.
17. Nimmon CC, Lee TY, Britton KE, Granowska M, Gruenewald S. Practical application of deconvolution techniques to dynamic studies. In: *Medical Radionuclide Imaging.* Vienna, Austria: IAEA; 1981:IAEA-SM-247/26 I:367–388.
18. Britton KE, Nimmon CC, Whitfield HN, Kelsey Fry I, Hendry WF, Wickham JEA. The evaluation of obstructive nephropathy by means of parenchymal retention functions. In: Hollenberg NK, Lange S, eds. *Radionuclides in Nephrology.* Stuttgart, Germany: Georg Thieme; 1980:151–154.
19. Kuruc A, Caldicott WJH, Treves S. An improved deconvolution technique for the calculation of renal retention functions. *Comput Biomed Res.* 1982;15:46–56.
20. Kuruc A, Treves S, Parker JA. Accuracy of deconvolution algorithms assessed by simulation studies: concise communication. *J Nucl Med.* 1983;24:258–263.
21. Sutton DG, Kemp V. Constrained least squares restoration and renogram deconvolution: a comparison by simulation. *Phys Med Biol.* 1992;37:53–67.
22. Russell CD, Japanwalla M, Khan S, Scott JW, Dubovsky EV. Techniques for measuring renal transit times. *Eur J Nucl Med.* 1995;22:1372–1378.
23. Nimmon CC, McAlister JM, Hickson B, Cattell WR. Study of the post-equilibrium slope approximation in the calculation of glomerular filtration rate using  $^{51}\text{Cr}$ -EDTA single injection technique. In: *Dynamic Studies with Radioisotopes in Medicine 1974.* Vienna, Austria: IAEA; 1975:249–256.
24. Blafox MD, Britton KE, Nimmon CC, Wedeen RP. The radionuclide renogram. In: Blafox MD, ed. *Evaluation of Renal Function and Disease with Radionuclides.* Basel, Switzerland: Karger; 1989:98–129.
25. Peters AM, Allison H, Ussov WY. Measurement of the ratio of glomerular filtration rate to plasma volume from the technetium-99m diethylene triamine penta-acetic acid renogram: comparison with glomerular filtration rate in relation to extracellular fluid volume. *Eur J Nucl Med.* 1994;21:322–327.